148 *Inorg. Chem.* **1994**, *33*, 148–156

Magnetic Circular Dichroism Studies of $[MOCl_4]^-$ (M = Cr, Mo, W) Chromophores: Assignment of Ligand Field and Charge Transfer States

Dawn M. Sabel and Andrew A. Gewirth[*]

Department of Chemistry, University of Illinois, 505 S. Mathews Avenue, Urbana, Illinois 61801

Received October 16, 1992[●]

Magnetic circular dichroism spectra were obtained for $[MOCl_4]^-$ (M = Cr, Mo) and $[WOCl_4(H_2O)]^-$ compounds. All of the spectra display temperature and field dependence consistent with a paramagnetic ground state. The two lowest energy bands are assigned to the $d_{xy} \rightarrow d_{xz},d_{yz}$ and $d_{xy} \rightarrow d_{x^2-y^2}$ ligand field transitions. All of the compounds display vibronic structure on the $d_{xy} \rightarrow d_{xz},d_{yz}$ band arising from coupling with the totally symmetric M–O stretch. The third band is assigned to a b_1(Cl) to $b_2(d_{xy})$ charge transfer transition and at slightly higher energies are charge transfer transitions from orbitals with e symmetry to the half-occupied d_{xy} orbital. The low energy of the b_1 to b_2 charge transfer band provides a consistent explanation of the inverted EPR parameters found in these complexes and in molybdenum-containing hydroxylases.

I. Introduction

The Mo active site in the Mo hydroxylases has been a focus of study ever since the initial work of Bray demonstrated that Mo was a necessary component of these proteins.[1-5] Although there have been many studies involving molybdenum enzymes in recent years, the nature of the molybdenum active site is not well-understood.[6-8] Degradation,[9-13] EXAFS,[8,14,15] and EPR[8,16] studies have been performed on a number of molybdenum enzymes, yet uncertainty involving the number, type, and geometry of the ligands in the Mo active site persists.

Optical study of the Mo hydroxylases has been hindered by the presence of strongly absorbing chromophores in the enzyme, usually an iron-containing moiety, and removal of these chromophores is difficult. In an attempt to circumvent this problem, Thomson and co-workers[17] performed low-temperature magnetic circular dichroism (MCD) spectroscopy on desulfo inhibited xanthine oxidase and subtracted the temperature dependent signal from the temperature independent MCD signal to yield the Mo(V) contribution. While a spectrum was obtained, insight was limited. This limited insight extends to recent MCD studies of DMSO reductase,[18,19] a Mo-containing enzyme which contains no other chromophores, in part because of a lack of knowledge about the spectroscopy of Mo(V) chromophores in general.

Due to the problems outlined above, molybdenum model complexes have been used extensively to obtain insight into the structure and reactivity of the molybdenum active site. The most studied systems involve the $[MOX_4]^-$ chromophores, where M is Cr, Mo, or W and X is Cl, Br, or SPh. These compounds have the advantage of being paramagnetic,[20-22] having known crystal structures,[20,23-28] and having the ability to be reduced and/or oxidized.[29-34] Although these compounds are well characterized structurally, their electronic structure remains a matter of much controversy. It is generally agreed that the energy ordering of the ligand field is $d_{xy} < d_{xz},d_{yz} < d_{x^2-y^2} < d_{z^2}$ with the unpaired electron in the d_{xy} orbital,[20,35-37] yet the energy of transitions between these orbitals is not clear. Much work has been done on the analogous VO^{2+} systems, including $[VOCl_4]^{2-}$, where it has been possible to give a consistent assignment of the ligand field transitions (ref 38 and references therein). Recent

---

[*] To whom correspondence should be addressed.

[●] Abstract published in *Advance ACS Abstracts,* December 1, 1993.

(1) Bray, R. C.; Malstrom, B. G.; Vanngard, T. *Biochem. J.* **1959**, *78*, 193.
(2) Bray, R. C. *Biochem. J.* **1961**, *81*, 196.
(3) Palmer, G.; Bray, R. C.; Beinert, H. *J. Biol. Chem.* **1964**, *239*, 2667.
(4) Bray, R. C.; Palmer, G.; Beinert, H. *J. Biol. Chem.* **1964**, *239*, 2667.
(5) Hing, T. E.; Mason, H. S.; Morrison, M., Eds. *Oxidases and Related Redox Systems*; John Wiley & Sons: New York, 1965; Vol. 1; p 359.
(6) Hanson, G. R.; Brunette, A. A.; McDonell, A. C.; Murray, K. S.; Wedd, G. S. *J. Am. Chem. Soc.* **1981**, *103*, 1953.
(7) Burgmayer, S. J. N.; Stiefel, E. I. *J. Chem. Educ.* **1985**, *62*, 943.
(8) Coughlan, M. P., Ed. *Molybdenum and Molybdenum-Containing Enzymes*; Pergamon Press: New York, 1980.
(9) Johnson, J. L.; Hainline, B. E.; Rajagopalan, K. V. *J. Biol. Chem.* **1980**, *255*, 1783.
(10) Johnson, J. L.; Rajagopalan, K. V. *Proc. Natl. Acad. Sci. U.S.A.* **1982**, *79*, 6856.
(11) Johnson, J. L.; Hainline, B. E.; Rajagopalan, K. V.; Arison, B. H. *J. Biol. Chem.* **1984**, *259*, 5414.
(12) Kramer, S. P.; Johnson, J. L.; Ribeiro, A. A.; Millington, D. S.; Rajagopalan, K. V. *J. Biol. Chem.* **1987**, *262*, 16357.
(13) Gruber, S.; Kilpatrick, L.; Bastian, N. R.; Rajagopalan, K. V.; Spiro, T. G. *J. Am. Chem. Soc.* **1990**, *112*, 8179.
(14) Sykes, A. G., Ed. *Advances in Inorganic and Bioinorganic Mechanisms*; Academic Press: London, 1983; Vol. 2.
(15) Spence, J. T. *Coord. Chem. Rev.* **1983**, *48*, 59.
(16) Spiro, T., Ed. *Molybdenum Enzymes*; Wiley-Interscience: New York, 1985.
(17) Peterson, J.; Godfrey, C.; Thomson, A. J.; George, G. N.; Bray, R. C. *Biochem. J.* **1986**, *233*, 107.
(18) Benson, N.; Farrar, J. A.; McEwan, A. G.; Thomson, A. J. *FEBS* **1992**, *307*, 169.
(19) Finnegan, M. G.; Hilton, J.; Rajagopalan, K. V.; Johnson, M. K. *Inorg. Chem.* **1993**, *32*, 2616.
(20) Garner, C. D.; Hill, L. H.; Mabbs, F. E.; McFadden, D. L.; McPhail, A. T. *J. Chem. Soc., Dalton Trans.* **1977**, 1202.
(21) Garner, C. D.; Hillier, I. H.; Mabbs, F. E.; Taylor, C.; Guest, M. F. *J. Chem. Soc., Dalton Trans.* **1976**, 2258.
(22) Hare, C.; Bernal, I.; Gray, H. B. *Inorg. Chem.* **1962**, *1*, 831.
(23) Gahan, B.; Garner, C. D.; Hill, L. H.; Mabbs, F. E.; Hargrave, K. D.; McPhail, A. T. *J. Chem. Soc., Dalton Trans.* **1977**, 1726.
(24) Garner, C. D.; Hill, L. H.; Mabbs, F. E.; McFadden, D. L.; McPhail, A. T. *J. Chem. Soc., Dalton Trans.* **1977**, 853.
(25) Scane, J. G. *Acta Crystallogr.* **1967**, *23*, 85.
(26) Bradbury, J. R.; Mackay, M. F.; Wedd, A. G. *Aust. J. Chem.* **1978**, *31*, 2423.
(27) Hill, L. H.; Howlader, N. C.; Mabbs, F. E.; Hursthouse, M. B.; Malik, K. M. *J. Chem. Soc., Dalton Trans.* **1980**, 1475.
(28) Bino, A.; Cotton, F. A. *Inorg. Chem.* **1979**, *18*, 2710.
(29) Bradbury, J. R.; Masters, A. F.; McDonell, A. C.; Brunette, A. A.; Bond, A. M.; Wedd, A. G. *J. Am. Chem. Soc.* **1981**, *103*, 1959.
(30) Ward, B. G.; Stafford, F. E. *Inorg. Chem.* **1968**, *7*, 2569.
(31) Gibson, V. C.; Kee, T. P.; Shaw, A. *Polyhedron* **1988**, *7*, 579.
(32) Fowles, G. W. A.; Frost, J. L. *J. Chem. Soc. A* **1967**, 671.
(33) Levason, W.; Narayanaswamy, R.; Ogden, J. S.; Rest, A. J.; Turff, J. W. *J. Chem. Soc., Dalton Trans.* **1981**, 2501.
(34) Mohammed, A. K.; Maverick, A. W. *Inorg. Chem.* **1992**, *31*, 4441.
(35) Gray, H. B.; Hare, C. R. *Inorg. Chem.* **1962**, *1*, 363.
(36) Collison, D. *J. Chem. Soc., Dalton Trans.* **1990**, 2999.
(37) Nugent, W. A.; Mayer, J. M. *Metal-Ligand Multiple Bonds*; Wiley-Interscience: New York, 1988.
(38) Collison, D.; Gahan, B.; Garner, C. D.; Mabbs, F. E. *J. Chem. Soc., Dalton Trans.* **1980**, 667.

0020-1669/94/1333-0148$04.50/0

work by Deeth has also provided a theoretical basis for the VO^{2+} assignments.[39] However, complications arise if the lowest lying charge transfer transitions obscure the higher energy ligand field promotions, as they do for the compounds considered here.

To investigate the nature of the bonding in these complexes, single-crystal EPR spectra for $[CrOCl_4]^-$ and $[MoOCl_4]^-$ have been obtained.[20,21] For both these complexes, $g_\parallel$ is near the free electron value of 2.0023. g value calculations made using the assigned b_2 (d_{xy}) to b_1 ($d_{x^2-y^2}$) transition have not been consistent with the observed values of g_z ($g_\parallel$). This indicates that either the oxotetrahalides have an especially large amount of covalent delocalization or that charge transfer bands arising from $^2B_1$ excited states may have low energies and need to be included in the calculations to account for the high values of $g_\parallel$ observed.[40–43] Unfortunately, there are no definitive assignments of any CT transition in this series of complexes. Values obtained for $g_\perp$ (g_{xy}), while lower than $g_\parallel$, are also close to the free electron value and also suggest that charge transfer transitions may need to be considered in calculations of this value.

In this work we utilize MCD spectroscopy to assign the electronic spectra of the $[MOCl_4]^-$ complexes. This information is then used to interpret the EPR parameters and bonding in these compounds.

II. Experimental Section

Synthesis. All manipulations were performed under an atmosphere of purified argon using standard Schlenk techniques. Oxalic acid and ammonium oxalate were recrystallized before use. Tetrapropylammonium bromide was dried *in vacuo* at 140 °C to remove any absorbed water. Ethanol, methanol, water, and ether were purified by standard techniques and degassed before use. All other reagents were used as received. Microanalyses were performed by the School of Chemical Sciences Microanalytical Laboratory, University of Illinois.

Tetrapropylammonium Tetrachlorooxochromate, $[Pr_4N][CrOCl_4]$. This compound was prepared by the method of Ziebarth and Selbin.[44] CrO_3 (33 mmol) was dissolved in glacial acetic acid (60 mL) saturated with HCl (g). Pr_4NBr (32 mmol) was dissolved in 30 mL of HCl-saturated glacial acetic acid and added dropwise to the above solution. The red-gold precipitate which immediately formed was isolated by filtration, rinsed with acetic acid/HCl(g) solution, and dried under vacuum in the presence of P_2O_5. Anal. Calcd for $C_{12}H_{28}NCrOCl_4$: C, 36.39; H, 7.13; N, 3.54; Cl, 35.81. Found: C, 36.42; H, 7.21; N, 3.65; Cl, 35.52.

Tetrapropylammonium Tetrachlorooxomolybdate, $[Pr_4N][MoOCl_4]$. This synthesis is based on a refinement of literature methods.[6] $Na_2MoO_4{\cdot}2H_2O$ (8.5 mmol) was reduced by the addition of hydrazine hydrate (40%, 16 mmol) in concentrated hydrochloric acid (45 mL) followed by heating to 80 °C for 3 h. The solution was cooled to −20 °C and then filtered. A solution of Pr_4NBr (9 mmol) dissolved in HCl (20 mL) was added dropwise to the filtrate at 90 °C. A light green precipitate formed immediately and was isolated by filtration. Recrystallization from methanol afforded green microcrystals which darkened to blue-green when dried *in vacuo* in the presence of P_2O_5. Anal. Calcd for $C_{12}H_{28}NMoOCl_4$: C, 32.75; H, 6.41; N, 3.18; Cl, 32.22; Mo, 21.80. Found: C, 32.75; H, 6.50; N, 3.17; Cl, 32.16; Mo, 21.78.

Tetrapropylammonium Aquatetrachlorooxotungstate, $[Pr_4N][WOCl_4(H_2O)]$. This compound was prepared using modified literature methods.[6,45] A solution of $[NH_4]_2[WOCl_5]$ (0.66 mmol) in HCl (9 mL) was stirred for 0.5 h and filtered.[45] The filtrate was heated to 40 °C and a solution of Pr_4NBr (0.8 mmol) in HCl (2 mL) was added dropwise. The solution was cooled to 0 °C, saturated with HCl gas, and stored overnight at −20 °C. The light blue microcrystals were isolated by filtration and dried over P_2O_5 *in vacuo*. Anal. Calcd for $C_{12}H_{30}NWO_2Cl_4$: C, 26.40; H, 5.54; N, 2.57; Cl, 25.97. Found: C, 26.18; H, 5.60; N, 2.52; Cl, 25.84.

Table 1. Selection Rules for Electronic Transitions

state transition	polarization[a]		MCD sign
	xy	*z*	
C_{4v}			
$^2B_2 \rightarrow {}^2A_1$	F(E)	F(B_2)	–
$^2B_2 \rightarrow {}^2A_2$	F(E)	F(B_1)	–
$^2B_2 \rightarrow {}^2B_1$	F(E)	F	+
$^2B_2 \rightarrow {}^2B_2$	F(E)	A(A_1)	+
$^2B_2 \rightarrow {}^2E$	A(A_1,B_1,B_2)	F(E)	+/–
C_{4v}'			
$\Gamma_7 \rightarrow \Gamma_6$	A	F(Γ_3,Γ_4,Γ_5)	–
$\Gamma_7 \rightarrow \Gamma_7$	A	A	+

[a] Key: F, forbidden; A, allowed. States in parentheses indicate enabling modes.

MCD Spectra. The MCD and CD spectra were obtained on a spectrometer built in our laboratory. Light from a xenon arc lamp or a tungsten–halogen lamp is monochromatized by a Cary 14 spectrometer modified with the addition of stepper motor control of wavelength drive and slit width. Wavelength calibration is performed prior to each experiment using the 435.8-nm line of an integral low-pressure Hg vapor lamp. The monochromatic light is collimated and transmitted though a Glan–Thompson prism polarizer and a photoelastic modulator (Hinds International). The beam is focused onto the sample in an Oxford Instruments SM4-7T split pair superconducting optical cryomagnet and detected by a photomultiplier tube having either a S-1 or S-20 response (Hamamatsu Photonics). The dc component of the resultant signal is used to maintain constant signal level by feedback to the phototube dynode voltage. The ac component is sent to a lock-in amplifier (Stanford Research Systems, SR510) which detects the circular dichroism (CD) signal and sends it to a computer. The CD sign and intensity was calibrated with *d*-10-camphorsulfonic acid prior to use.[46] MCD operation and sign were confirmed by obtaining spectra of $K_3Fe(CN)_6$.[47]

Samples were prepared as Nujol or poly(dimethylsiloxane) mulls sealed between quartz disks. All preparation was done in a glovebox and the sample cell was quickly transferred into the MCD spectrometer. The MCD spectra were obtained at 4.2 K and various field strengths. Baseline CD (0 T) spectra were collected and subtracted from the MCD data. All of the MCD spectra were collected with the exit slit of the monochromator having a fixed width. With a slit separation of 1.5 mm, the effective bandwidth ranged from 450 cm^{-1} at 40 000 cm^{-1} to 87 cm^{-1} at 11100 cm^{-1}. Spectra were also collected with 0.5- and 0.75-mm slits where the effective bandwidth ranged from 100 cm^{-1} at 25 000 cm^{-1} to 30 cm^{-1} at 11 100 cm^{-1} for 0.5-mm slits and from 151 cm^{-1} at 25 000 cm^{-1} to 35 cm^{-1} at 11 100 cm^{-1} for 0.75-mm slits.

III. Results

1. Optical Spectra. The $[MOCl_4]^-$ ions display C_{4v} symmetry with the unpaired electron in the d_{xy} orbital which gives rise to a $^2B_2$ ground state. Assignment of the transitions from this $^2B_2$ ground state is made with reference to selection rules summarized in Table 1. There are several levels of analysis of the transitions. The electric dipole operator alone enables two transitions: excitation to $^2B_2$ in z polarization and to ^2E in xy polarization. All other absorptions are electric dipole forbidden. If vibronic coupling is included in the selection rules, then transitions to all excited states are allowed in xy polarization and only transitions to $^2B_1$ excited states are uniquely forbidden in z. By way of contrast, if spin–orbit coupling is considered, the C_{4v}' double group gives a Γ_7 ground state with Γ_6 and Γ_7 excited states. Transitions from Γ_7 to excited states with either of these symmetries are electric dipole allowed in at least one polarization. In situations where either vibronic or spin–orbit coupling effects are large, as they are in the Mo (λ = 900 cm^{-1})[48] and W (λ = 2700 cm^{-1})[48] complexes considered in this paper, it is clear that assignments on the basis of polarized optical spectra alone are not likely to be unequivocal. Indeed, ambiguity of assignments for ligand field and charge transfer transitions for these complexes has been a hallmark ever since the first attempts 30 years ago.[35]

---

(39) Deeth, R. J. *J. Chem. Soc., Dalton Trans.* **1991**, 1467.
(40) Sunil, K. K.; Harrison, J. F.; Rogers, M. T. *J. Chem. Phys.* **1982**, *76*, 3087.
(41) Kon, H. E.; Sharpless, N. E. *J. Chem. Phys.* **1965**, *42*, 906.
(42) Kon, H. E.; Sharpless, N. E. *J. Phys. Chem.* **1966**, *70*, 105.
(43) Manoharan, P. T.; Rogers, M. T. *J. Chem. Phys.* **1968**, *49*, 5510.
(44) Ziebarth, O.; Selbin, J. *Inorg. Nucl. Chem.* **1970**, *32*, 849.
(45) Collenberg, O. *Z. Anorg. Allg. Chem.* **1918**, *102*, 247.
(46) Chen, G. C.; Yang, J. T. *Anal. Lett.* **1977**, *10*, 1195.
(47) Schatz, P. N.; McCaffery, A. J.; Suetaka, W.; Henning, G. N.; Ritchie, A. B. *J. Chem. Phys.* **1966**, *45*, 722.
(48) Goodman, B. A.; Raynor, J. B. *Adv. Inorg. Chem. Radiochem.* **1970**, *13*, 135.

MCD gives rise to additional selection rules which simplify assigning transitions in these complexes. These are $\Delta m_J = \pm 1$ for positive or negative MCD sign, respectively, and $\Delta m_s = 0$. We use group theory to consider case-by-case the MCD selection rules for the individual transitions. First, we consider transitions from $^2B_2$ to ^2E which are electric dipole allowed in xy polarization. Spin–orbit coupling within the e manifold splits the pair by an energy equal to λ, the spin–orbit coupling constant, giving two components in C_{4v}': Γ_6 with $|m_J| = {}^1/_2$ and Γ_7 with $|m_J| = 3/2$. The d_{xy} ground state in C_{4v}' transforms as Γ_7 with $|m_J| = {}^1/_2$. Application of a magnetic field splits this Kramers doublet into two levels separated by $g\beta H$. At room temperature, both m_J levels of the Kramers doublet ground state are approximately equally populated and MCD transitions from both of these levels will have equal intensity but opposite sign. This means that there will be no net MCD at room temperature. As the temperature is lowered, more population will accrue to the $m_J = {}^1/_2$ level, giving rise to a temperature-dependent MCD signal known as a *C* term.[49] At 4.2 K and 6 T, the $m_J = {}^1/_2$ level of the ground state will contain approximately 85% of the unpaired electron population if $g = 2$. This means that the Γ_7 to Γ_6(e) transition will exhibit a negative *C* term, while the Γ_7 to Γ_7(e) transition will have a positive *C* term. Since Γ_6 and Γ_7 are separated in energy by λ, transitions from $^2B_2$ to ^2E will exhibit derivative-shaped bands, known as pseudo-*A* terms.[49] The $^2A_1$ and $^2A_2$ states transform as Γ_6 in C_{4v}' symmetry. Following the above argument, promotion to $^2A_1$ or $^2A_2$ excited states will exhibit negative *C* terms. Analogously, transitions to the $^2B_1$ or $^2B_2$ excited states, which transform as Γ_7 in C_{4v}', will show positive *C* terms. These selection rules are shown in Table 1.

2. MCD Spectra. All bands exhibit temperature and field dependence consistent with their origin from MCD *C* terms which is expected as these complexes are paramagnetic with one unpaired electron.[22] Simultaneous Gaussian resolution of the MCD spectra was performed using the Levenberg–Marquardt method[50] and the minimum number of Gaussians possible. Bandwidths were estimated from the spectra with the only restriction being that the two portions of a pseudo-*A* term must have bandwidths that differ by less than 10%. In all cases, the difference in intensity between the Gaussian and experimental spectra was less than 10% of the actual MCD intensity in the simulated regions.

The spectra from these centers are best understood by reference to the molecular orbital diagrams (Figure 1) predicted from DVXα calculations.[51,52] The orbital diagram is divided into two main parts. At high energy, above the half-occupied $2b_2$ (d_{xy}) orbital, are the remaining three ligand field orbitals; below the d_{xy} orbital are ligand-based orbitals. The Cl orbitals are anticipated to be closer in energy to those from the metal center than the O orbitals[53] and this is indeed predicted in both the DVXα and MSXα calculations.[51,52,54] In the case of $[WOCl_4(H_2O)]^-$, DVXα calculations on the analogous Mo compound predict the axial aqua MOs to appear below the equatorial ligand level,[52] and hence they do not appear in the energy range studied here. The Cl orbitals may be divided into nonbonding and bonding sets, with the nonbonding set higher in energy. The MO diagrams thus indicate that transitions from the ligand orbitals to the half-occupied d_{xy} orbital, and transitions from d_{xy} to the higher lying ligand field states may occur at approximately the same energies. This ambiguity of energy of ligand field and charge transfer excited states has substantially complicated previous assignments in these complexes.[36,55-58]

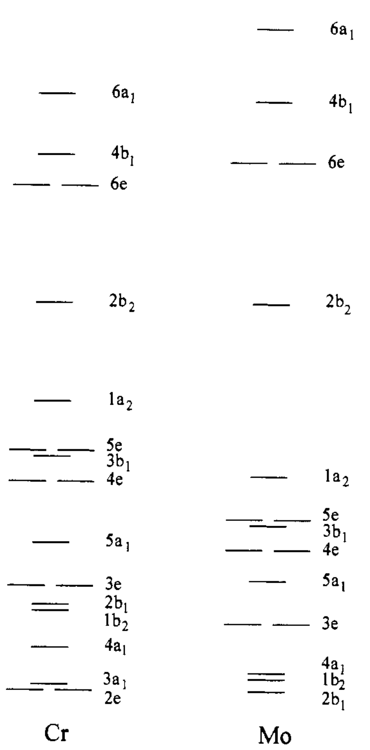

Figure 1. Molecular orbital diagram for $[CrOCl_4]^-$ and $[MoOCl_4]^-$ as determined by DVX calculations.[51,52]

2.1. $[MoOCl_4]^-$. The tetrapropylammonium salts of the $[MOCl_4]^-$ compounds were used to avoid possible interference arising from cation-based transitions in the ultraviolet region of the spectra. While crystal structures for the three tetrapropylammonium compounds studied here have not been obtained, comparison of the crystal structures for $[Ph_4As][MoOBr_4(H_2O)]$ (space group *P*4/*n*)[25] and $[NEt_4][MoOBr_4(H_2O)]$ (space group *Pnma*)[28] indicates that the $[MoOBr_4(H_2O)]^-$ moiety is slightly distorted from C_{4v} symmetry when precipitated with less bulky ammonium cations. When distorted, the $[MoOBr_4(H_2O)]^-$ ion has two different Mo–Br bond lengths that differ by 0.007 Å and a mirror plane that bisects the Br–Mo–Br angle, and the O–Mo–O bond angle is 178°. This distortion places the oxygen slightly closer to the more tightly bound Br. This effect will be addressed in more detail in the discussion section.

Figure 2a shows the MCD of $[Pr_4N][MoOCl_4]$ obtained at 4.2 K and 2 and 6 T. The spectrum is composed of a number of bands, some overlapping, which are numbered from lower to higher energy. The spectral origin of each is discussed in the analysis section.

The lowest energy band exhibits both positive and negative MCD intensity centered at ca. 16 000 cm^{-1}. The MCD intensity is not evenly distributed between the positive and negative components as the lower energy negative side is almost a factor of two more intense and exhibits vibronic features. The next feature, band 2, is centered at 23 900 cm^{-1} and has positive MCD intensity approximately equal to the previous band. Although these bands are far from each other in energy, there is measurable MCD intensity between them. The magnitude of this sloping MCD intensity is independent of sample and the intensity is not present in base-line MCD spectra obtained missing only the actual sample. More detailed inspection of this region did not reveal

---

(49) Piepho, S. B.; Schatz, P. N. *Group Theory in Spectroscopy with Applications to Magnetic Circular Dichroism*; John Wiley & Sons: New York, 1983.
(50) Press, W. H. *Numerical Recipes*; Cambridge University Press: Cambridge, England, 1986; p 526.
(51) Deeth, R. J. *J. Chem. Soc., Dalton Trans.* **1990**, 365.
(52) Deeth, R. J. *J. Chem. Soc., Dalton Trans.* **1991**, 1895.
(53) Winkler, J. T.; Gray, H. B. *Comments Inorg. Chem.* **1981**, *1*, 257.
(54) Weber, J.; Garner, C. D. *Inorg. Chem.* **1980**, *19*, 2206.
(55) Piovesana, O.; Furlani, C. *Inorg. Nucl. Chem. Lett.* **1967**, *3*, 535.
(56) Collison, D. *J. Chem. Soc., Dalton Trans.* **1989**, 1.
(57) Garner, C. D.; Kendrick, J.; Lambert, P.; Mabbs, F. E.; Hillier, I. H. *Inorg. Chem.* **1976**, *15*, 1287.
(58) Garner, C. D.; Hillier, I. H.; Kendrick, J.; Mabbs, F. E. *Nature* **1975**, *258*, 138.

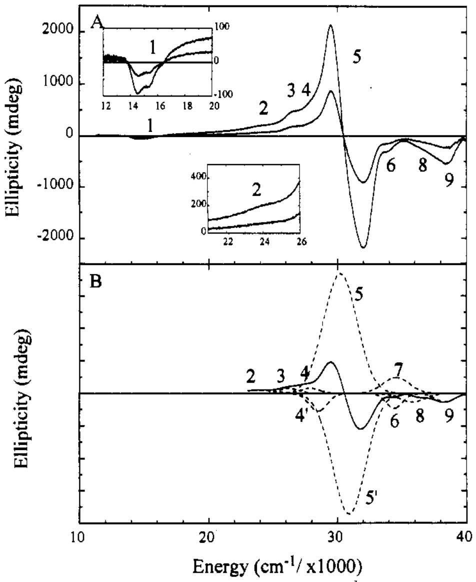

Figure 2. (A) MCD spectrum of [Pr$_4$N][MoOCl$_4$] in poly(dimethylsiloxane) at 4.2 K and 2 and 6 T with 1.5-mm slits. The inserts show two parts of the low-energy portion of this spectrum and were collected with 0.5-mm slits. (B) Gaussian-resolved spectrum of [Pr$_4$N][MoOCl$_4$]. The dashed lines represent the individual Gaussians used in the fit and are numbered from low to high energy with primed numbers indicating the high-energy portion of a ^{2}E excited state.

any additional transitions and possible sources of this intensity will be addressed below.

At 26 300 cm^{-1} another positive feature (band 3) is observed which is more intense than the previous two bands and appears to be a sharper transition. Slightly higher in energy (ca. 27 500 cm^{-1}) is a positive sloping band (4) which leads into the dominant transition of the spectrum, the intense derivative transition (band 5) centered at ca. 31 000 cm^{-1}. Band 5 is at least four times as intense as the other transitions observed and close inspection reveals that the positive portion of the derivative band is narrower than the negative region. However, the positive and negative regions have approximately equal intensity.

The next feature in this spectrum is the negative band at ca. 34 000 cm^{-1} followed by the broad negative band at ca. 38 000 cm^{-1}. Both of these bands are approximately as intense as the features from 22 000–27 000 cm^{-1}.

2.2. [CrOCl$_4$]$^-$. In order to verify assignments for the Mo complex and to provide additional insight into the excited state spectral features, we obtained MCD spectra of the analogous Cr and W complexes. Figure 3a shows the MCD spectrum of [Pr$_4$N]-[CrOCl$_4$]. All the features observed in the [MoOCl$_4$]$^-$ spectrum are also seen in the [CrOCl$_4$]$^-$ spectrum but at consistently lower energies. Additional MCD features are observed at energies above 31 000 cm^{-1}.

The lowest energy band is centered at 13 500 cm^{-1} and has both positive and negative MCD components (see inset Figure 3a). The negative component is more intense than the positive feature and both display a significant amount of vibronic structure which is similar to features seen in the Mo spectrum. Band 2, the weak positive transition at 17 600 cm^{-1}, occurs at much lower energy than observed for the Mo case. Unlike the [MoOCl$_4$]$^-$ spectrum, there is no featureless MCD intensity between these bands due to the fact that they lie close in energy.

The feature at ca. 18 900 cm^{-1} represents the first relatively intense transition and has a positive MCD sign consistent with the Mo case above. Again, there is a positive shoulder (band 4) at approximately 21 000 cm^{-1} which leads into the dominant derivative-shaped band 5. In contrast to the Mo case, band 4 appears to occur over a larger energy range and does not overlap as much with band 5.

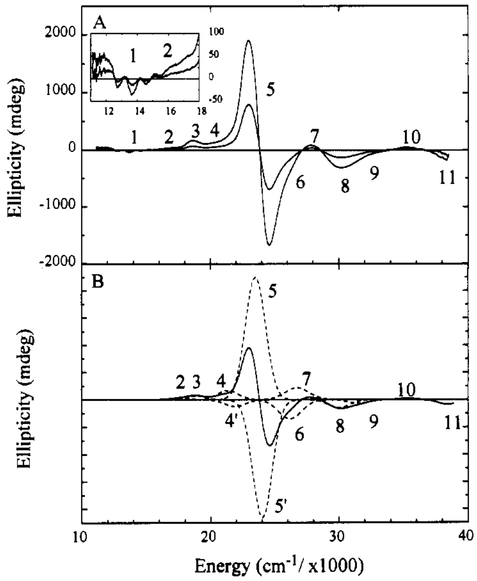

Figure 3. (A) MCD spectrum of [Pr$_4$N][CrOCl$_4$] in Nujol at 4.2 K and 2 and 6 T with 1.5-mm slits. The low energy portion of the spectrum (insert) was obtained with 0.5-mm slits. (B) Gaussian-resolved spectrum of [Pr$_4$N][CrOCl$_4$]. The dashed lines represent the individual Gaussians used in the fit and are numbered from low to high energy with primed numbers indicating the high energy portion of a ^{2}E excited state.

As with [MoOCl$_4$]$^-$, the [CrOCl$_4$]$^-$ spectrum is dominated by band 5 at 23 700 cm^{-1}. The positive and negative portions of this band again have similar intensities, however the line widths of the two components of this band are comparable, unlike the [MoOCl$_4$]$^-$ case. The sharp negative shoulder present in the Mo spectrum has broadened in the [CrOCl$_4$]$^-$ spectrum and is centered at ca. 26 000 cm^{-1}. In contrast to the Mo spectrum, the Cr spectrum exhibits a weak positive MCD feature at ca. 27 000 cm^{-1}. This is followed by a broad negative band at 30 000 cm^{-1} which was also observed for Mo.

At 35 000 cm^{-1} there is a very weak positive band observed that was not present for Mo. Likewise, the negative band at ca. 38 000 cm^{-1} was not seen in the previous spectrum. This is most certainly due to the lower transition energies expected for the Cr complex and these transitions occur at higher energies than probed here for the Mo complex.

2.3. [WOCl$_4$(H$_2$O)]$^-$. The aqua complex was used due to the difficulty in preparing [WOCl$_4$]$^-$. The MCD spectrum of [WOCl$_4$(H$_2$O)]$^-$ is presented in Figure 4a. As in the previous two cases, the spectrum is dominated by an intense, derivative-shaped band. The spectrum is similar to that of [MoOCl$_4$]$^-$ with the intense transitions shifted to higher energies.

The lowest energy transition centered at 15 300 cm^{-1}, has both positive and negative features. The derivative shape of this transition is more apparent for the W complex than in the Mo and Cr cases and the vibronic features are more pronounced. At ca. 26 000 cm^{-1} there is a weak positive band analogous to that for the Mo complex. There is also MCD intensity between the first two transitions as was the case in the Mo spectrum. The third feature in the spectrum (band 3) occurs at ca. 32 000 cm^{-1} and is more intense than the previous two bands. In contrast to the Mo and Cr cases, there does not appear to be a shoulder present between band 3 and the dominant derivative band centered at ca. 37 000 cm^{-1}. Band 5 is broader than both the Mo and Cr cases, and the positive portion is less intense and slightly less broad than the negative region.

IV. Analysis

1. Band Assignments. The Gaussian resolved spectra for [MoOCl$_4$]$^-$, [CrOCl$_4$]$^-$, and [WOCl$_4$(H$_2$O)]$^-$ are shown in Figures 2b, 3b, and 4b, respectively. All the spectra are composed of a

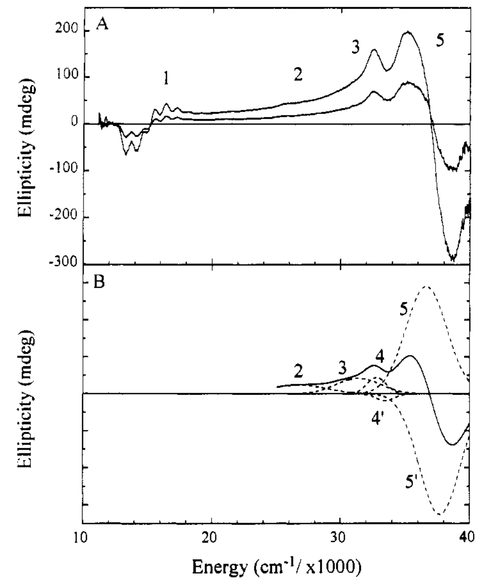

Figure 4. (A) MCD spectrum of $[Pr_4N][WOCl_4(H_2O)]$ in poly(dimethylsiloxane) at 4.2 K and 2 and 6 T with 1.5-mm slits. (B) Gaussian-resolved spectrum of $[Pr_4N][WOCl_4(H_2O)]$. The dashed lines represent the individual Gaussians and are numbered from low to high energy with primed numbers indicating the high-energy portion of a ^2E excited state.

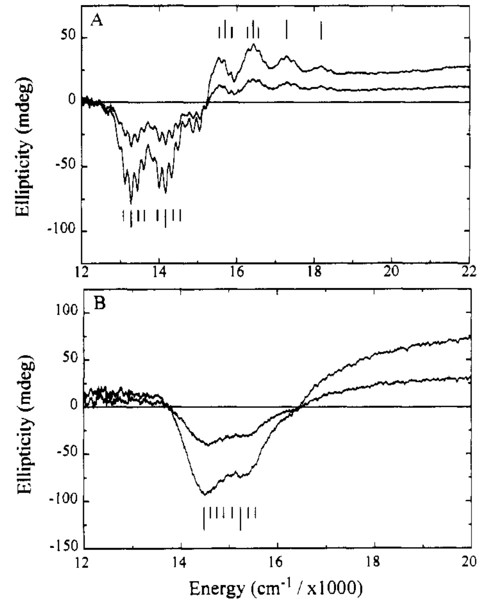

Figure 5. High-resolution MCD spectrum of the low-energy region for (A) $[Pr_4N][WOCl_4(H_2O)]$ and (B) $[Pr_4N][MoOCl_4]$in poly(dimethylsiloxane) at 4.2 K and 4 T. The W spectrum was collected with 0.75-mm slits, and the Mo spectrum, with 0.5-mm slits. Solid lines indicate separation of individual vibronic components as discussed in the text.

number of overlapping bands which are numbered from lower to higher energy. Band 1 was not used in the Gaussian fitting procedure due to the considerable vibronic structure present in all three cases.

Band 1 exhibits both positive and negative MCD intensity and is centered at ca. 13 500, 16 000, and 15 300 cm^{-1} for the Cr, Mo, and W complexes, respectively. Because both MCD signs are observed, this feature is assigned as a pseudo-*A* term deriving from a $^2B_2 \rightarrow {}^2E$ transition. Literature absorption spectra are also consistent with this assignment as the transition is almost entirely *xy* polarized.[24,36,53,56] All of the MCD spectra exhibit vibronic features on band 1 (Figures 3a and 5), congruent with similar features observed in the absorption spectra.[24,36,53,56] The low energy of the band along with its vibronic component and weak intensity relative to the rest of the spectrum implies that it originates from a ligand field transition. This is consistent with the assignment of this band as deriving from the $2b_2$ (d_{xy}) to 6e (d_{xz},d_{yz}) orbital transition, in agreement with previous studies.[24,35,36,53,56] The existence of a pseudo-*A* term associated with this transition makes its assignment as a ^2E excited state unequivocal. The asymmetry of band 1 and the origin of the vibronic structure will be addressed below.

In the case of $[WOCl_4(H_2O)]^-$, the derivative shape is much more apparent than in the Mo and Cr cases and the vibronic features are more pronounced. This may be due to the large value of the spin orbit coupling constant for W(V) (2700 cm^{-1})[48] compared to the magnitude of the vibronic progression (890 cm^{-1}). From the spectrum, the effective spin–orbit coupling constant for the transition is estimated at 2250 cm^{-1}. This may be used to ascertain the relative amounts of W and O (λ = 158 cm^{-1})[59] character in this excited state by assuming that the splitting is divided over contributions from the metal and ligand. For $[WOCl_4(H_2O)]^-$, we obtain ca. 80% metal character in the ^2E excited state, indicating that covalent delocalization is relatively unimportant in this complex.

Band 2 is observed at 17 550, 23 900, and 26 700 cm^{-1} for the Cr, Mo, and W complexes, respectively, and is approximately as intense as band 1 in both the MCD and previous absorption spectra.[24,36,53,56] A $^2B_1$ or $^2B_2$ excited state is inferred from the positive MCD sign (Table 1). The next ligand field transition expected would be to the $d_{x^2-y^2}$ orbital, which transforms as B_1 in C_{4v}. Polarized absorption studies reveal that band 2 is more intense in *xy* than *z* polarization which is consistent with a $^2B_1$ excited state.[36,53,56] The $^2B_2$ to $^2B_1$ transition is forbidden in *z* polarization under both electric dipole and vibronic selection rules. That this feature exhibits intensity in *z* polarization in the absorption spectrum may be due to the effect of spin orbit coupling, which is expected to be large in states which are metal-centered and would make this transition allowed in *z* polarization (Table 1). Collison[36,56] and Gray[53] have also assigned this band to the $^2B_2$ to $^2B_1$ transition. The positive MCD sign of this band allows no other interpretation of its origin.

For both $[MoOCl_4]^-$ and $[WOCl_4(H_2O)]^-$ there is additional intensity observed between bands 1 and 2. We note that MCD spectra of $[AsPh_4][MoOCl_4]$ and $[PPh_4][MoOCl_4(H_2O)]$ obtained by Enemark also exhibit some positive MCD intensity in this region.[60] There are several possible origins of this behavior. First, the samples may be contaminated with a paramagnetic species which may have some intensity in this spectral region. This could also provide an explanation for the distorted band 1 observed in the Mo complex. However, the microanalytical data collected on these compounds do not indicate the presence of a contaminant. Second, contamination could occur as a result of the mulling processes. However spectra obtained using a different mulling agent (poly(dimethylsiloxane)) exhibit the same features as do spectra obtained using Nujol. Thus, the mulling agent is likely not the source of the positive MCD intensity between bands 1 and 2. A third possible source of intensity involves overlap of vibronic envelopes from both bands. While considerable vibronic structure has been observed on band 1 in optical absorption studies[24,36,53,56] and on the MCD here, vibrational structure was not observed on band 2. The vibrational envelopes of both bands 1 and 2 are relatively broad (3000–5000 cm^{-1}). Since band 2 and the positive portion of band 1 both transform as Γ_7 in C_{4v}', out-of-state spin–orbit coupling may occur, leading to intensity stealing. The mixing of these states may allow intensity to be gained in the vibrational features furthest from the transition origin and account for the MCD signal observed in the region

---

(59) McClure, D. S. *J. Chem. Phys.* **1949**, *17*, 905.
(60) Enemark, John H. University of Arizona. Private communication.

between these bands. Finally, intensity in the region between bands 1 and 2 could derive from the presence of another, unresolved transition. A complete understanding of the intensity in this spectral region will require an in-depth analysis of the vibronic structure present on band 1.

The negative lobe of band 1 is consistently more intense than the positive component for all three $[MOCl_4]^-$ complexes. This asymmetry could derive from several sources. First, it is possible that an additional transition is present which contributes negative *C* term intensity to the band. However, our observation of this effect for all three complexes makes this explanation unlikely as some movement of this putative transition relative to the ^2E excited state would be expected over the three different metals. A second possibility may derive from intensity stealing from other excited states of the same symmetry. The higher energy component is the one reduced in intensity and this may result from its being somewhat closer to the other states of Γ_7 symmetry, specifically $^2B_1$ ($d_{x^2-y^2}$). As the energy separation between this state and ^2E (d_{xz},d_{yz}) gets larger, band 1 should appear more symmetric, and indeed that is the case going from Cr to W. The intensity of Band 2 also reflects this change. For $[CrOCl_4]^-$, band 2 is much more intense than the positive portion of Band 1 while for $[MoOCl_4]^-$ the positive region of band 1 is not well-defined. By way of contrast, $[WOCl_4(H_2O)]^-$ displays comparable intensities between band 2 and the high-energy region of band 1. Finally, the $[MOCl_4]^-$ moieties may be slightly distorted as addressed above. However, the expected distortion has a dihedral mirror plane; hence, this does not lead to improved overlap between the ground and excited state orbitals, and no intensity variations are expected.

The third feature in the MCD spectra is centered at 18 900, 26 200 and 31 400 cm^{-1} for $[CrOCl_4]^-$, $[MoOCl_4]^-$, and $[WOCl_4(H_2O)]^-$, respectively. The positive MCD intensity again indicates that this is due to either a $^2B_2$ or $^2B_1$ excited state. There are no additional ligand field levels remaining with the appropriate symmetry implying that band 3 is due to a charge transfer transition. From Figure 1, the $3b_1$ to $2b_2$ excitation occurs in this energy range and has the proper symmetry to account for the positive MCD signal. The low-energy of this transition is not unexpected as the $3b_1$ orbital is essentially nonbonding because of the poor overlap between the $d_{x^2-y^2}$ and Cl p orbitals arising from the near 90° O–M–Cl bond angle ($[CrOCl_4]^-$, 104.5°; $[MoOCl_4]^-$, 105.2°).[23,24]

As in the case of band 2, the band 3 transition is both electric dipole and vibronically forbidden in *z* polarization. However, *z*-polarized absorption intensity has been observed at energies slightly offset from the *xy*-polarized signal.[36,56] There are two possible sources of this intensity. First, spin–orbit coupling could mix in *z* intensity. If this is the case, the amount of spin–orbit coupling will be manifested in the ratio between the MCD and absorption intensities (*C*/*D*). For $[MoOCl_4]^-$ the *C*/*D* ratio is anticipated to be lower for band 3 (ligand-based transition) than band 2 (metal-based transition) because of the lower spin–orbit contribution from the ligands. *C*/*D* ratios for $[MoOCl_4]^-$ were calculated using the MCD and literature absorption spectra[36] and confirm that the *C*/*D* ratio for band 3 is ca. 70% that for band 2. For $[CrOCl_4]^-$ the ligand has a larger spin–orbit coupling constant than the metal (587 vs 380 cm^{-1}),[48,59] implying that band 3 will have a larger *C*/*D* ratio than band 2. Using literature absorption spectra,[56] the *C*/*D* ratio for band 3 is 1.5 times that for band 2 consistent with spin–orbit coupling effects.

A second possibility is that additional *z*-polarized intensity may be gained if excitation to a $^2A_1$ or $^2A_2$ state occurs at approximately the same energy. Accidental overlap of transitions could be reflected in the 170- and 100-cm^{-1} separations between *xy*- and *z*-polarized absorption envelope origins for $[CrOCl_4]^-$ and $[MoOCl_4]^-$, respectively.[36,56] Unfortunately, polarized absorption spectra for $[WOCl_4(H_2O)]^-$ are not available since the presence of the axial aqua group would further separate the $^2A_2$ and $^2B_2$ states. MCD spectra, however, do not indicate a negative band in this region. Previously, Band 3 had been assigned to the $2b_2$ (d_{xy}) to $6a_1$ (d_{z^2}) ligand field excitation,[36,56] however the positive MCD sign observed here indicates that this transition alone is not responsible for the observed spectra.

At higher energy, band 4 appears as a flat feature between bands 3 and 5. While the positive sign seems to imply the presence of a $^2B_1$ or $^2B_2$ excited state, there are no states of proper symmetry in this energy range (Figure 1). Gaussian resolution of band 4 indicates that it is likely made up of positive and negative features (4 and 4′ in Figures 2b, 3b, and 4b) of a pseudo-*A* term deriving from a ^2E excited state. This transition is centered at 21 600, 28 200, and 33 100 cm^{-1} for the Cr, Mo, and W complexes, respectively. The negative portion is not directly observed due to overlap with higher energy transitions. Previous absorption studies in this region demonstrated that this transition has intensity in both *xy* and *z* polarizations consistent with the ^2E excited state.[36,56,57] There are several orbitals of proper symmetry that occur in this energy range (Figure 1) and this transition is assigned to the 5e to $2b_2$ (d_{xy}) promotion.

In-state spin–orbit splitting were obtained from the Gaussian resolved spectra for band 4 and found to have values of 554 cm^{-1} for $[CrOCl_4]^-$, 605 cm^{-1} for $[MoOCl_4]^-$, and 697 cm^{-1} for $[WOCl_4(H_2O)]^-$. All of these values vary from the free ion spin–orbit coupling constant for Cl (587 cm^{-1})[59] and reflect participation of the metal centers in the excited state. This deviation of the excited state splitting from the chlorine value is a direct indication of the amount of delocalization of electron density onto the metal center. While the exact magnitude of the splitting is dependent on the spectral fit, the calculated splitting is consistent with between 20% and 5% metal character present in the ^2E excited state.

Band 5 dominates the MCD spectra of all three complexes. Its derivative shape indicates the presence of a pseudo-*A* term and a transition to a ^2E excited state. This feature is centered at ca. 23 800, 30 500, and 37 300 cm^{-1} for the Cr, Mo, and W complexes, respectively, and is assigned to the 4e to $2b_2$ orbital transition. The low-energy positive portion of band 5 in the Mo and W spectra is less intense and has a narrower line width than the negative portion of this band. This is likely due to overlap of the positive lobe of band 5 with the negative part of band 4 discussed above. This band displays the most intensity in both absorption and MCD spectra.[35,57] This is due to the large overlap between the donating and accepting molecular orbitals. From the Gaussian resolved spectrum, λ_{eff} is estimated at 531 cm^{-1} for $[CrOCl_4]^-$, 669 cm^{-1} for $[MoOCl_4]^-$, and 836 cm^{-1} for $[WOCl_4(H_2O)]^-$. All of these transitions contain more metal character than the corresponding excited state in band 4, consistent with the greater intensity for this excitation.

The remaining portion of the spectrum is not easily understood due to the large amount of overlap between bands in the MCD spectrum and the absence of quantitative single crystal absorption work in the high energy region. From the Gaussian-resolved spectra for $[CrOCl_4]^-$ and $[MoOCl_4]^-$ (Figures 2b and 3b), band 6 occurs at 26 200 and 34 400 cm^{-1}, respectively. The negative intensity indicates transition to either a $^2A_1$ or $^2A_2$ excited state. From the MO diagrams (Figure 1), the most likely transitions in this energy range are $2b_2$ (d_{xy}) to $6a_1$ (d_{z^2}) and $5a_1$ to $2b_2$ (d_{xy}). While there is no experimental evidence to indicate which transition is responsible for this band, the ligand field transition to $6a_1$ (d_{z^2}) is tentatively assigned to this feature.

Band 7 is most evident in the $[CrOCl_4]^-$ spectrum (26 700 cm^{-1} in Figure 3) but is also present in the Gaussian-resolved spectrum of $[MoOCl_4]^-$ (34 500 cm^{-1} in Figure 2b). The positive sign indicates a $^2B_1$ or $^2B_2$ excited state. There are several possible charge transfer transitions that may give rise to this band including $2b_1$ to $2b_2$ (d_{xy}) and 5e to 6e excitations. However, it is not possible to make a definitive assignment.

Table 2

		Cr			Mo		
transition	band	DVXα[a]	MSXα[b]	MCD	DVXα[c]	MSXα[b]	MCD
$2b_2 \rightarrow 6e$	1	13 565	8 300	13 500	16 418	15 600	16 000
$2b_2 \rightarrow 4b_1$	2	16 724	19 400	17 550	22 627	23 300	23 900
$3b_1 \rightarrow 2b_2$	3	*d*	*d*	18 900	*d*	*d*	26 200
$5e \rightarrow 2b_2$	4	22 671	10 700	21 600	29 335	23 000	28 200
$4e \rightarrow 2b_2$	5	25 077	12 900	23 800	31 948	25 700	30 500
$2b_2 \rightarrow 6a_1$	6	23 757	26 600	26 200	31 165	37 000	34 400

[a] Reference 51. [b] Reference 54. [c] Reference 52. [d] Transition energy not calculated.

Bands 8 and 9 are both negative transitions at 30 000 and 31 500 cm^{-1}, respectively, for $[CrOCl_4]^-$ and 35 800 and 38 300 cm^{-1}, respectively, for $[MoOCl_4]^-$. The negative MCD intensity indicates the presence of $^2A_1$ or $^2A_2$ excited states. Other excited states are undoubtedly also present.

2. Vibronic Structure. A vibronic progression of ca. 890 cm^{-1} is observed on both components of band 1 in the $[WOCl_4(H_2O)]^-$ complex and similar, although less well resolved features are also observed in spectra of $[CrOCl_4]^-$ (930 cm^{-1}) and $[MoOCl_4]^-$ (900 cm^{-1}) (Figure 5). The unpolarized W absorption spectrum and the polarized single-crystal absorption spectra of the Cr and Mo complexes also display vibronic structure, however, it is more evident in xy than z polarization in these latter two systems. By reference to Table 1, a_1, b_1, and b_2 symmetry vibrations may enable the $^2E \leftarrow {}^2B_2$ electronic transition. The progression observed here is of the correct energy to be associated with the totally symmetric M–O stretching mode in the electronic excited state. The vibronic energies observed here are lower than the ground-state a_1 vibrational energies of 1019,[61] 1012,[62] and 980[36] cm^{-1} for $[CrOCl_4]^-$, $[MoOCl_4]^-$, and $[WOCl_4(H_2O)]^-$, respectively. This energy lowering is anticipated as the electronic transition promotes an electron into the d_{xz},d_{yz} antibonding orbitals, weakening the M–O bond. For Cr and Mo, the vibrational energies for the M–O stretch are greater than or on the order of the spin–orbit splitting between the Γ_6 and Γ_7 components of the excited state, which may distort the derivative shape of band 1. Due to this distortion, the magnitude of the in-state spin–orbit coupling can not be estimated directly from the spectra of these compounds.

The MCD spectrum of $[WOCl_4(H_2O)]^-$ has an additional vibrational feature at ca. 161 cm^{-1} intervals with analogous, although less intense, features present for $[MoOCl_4]^-$ with ca. 180 cm^{-1} progressions (Figure 5). The low energy of this progression indicates that this may be a bending mode, and similar progressions observed by Gray[53] in the $[MoOCl_4]^-$ compounds have been assigned to the totally symmetric O–M–Cl bending mode, which has a ground-state frequency of 184 cm^{-1}.[62] While the low-energy IR spectrum of $[WOCl_4(H_2O)]^-$ has not been assigned, it is not unreasonable to assign the features observed to an analogous bending mode.

V. Discussion

1. Ligand Field Transitions. Table 2 summarizes the MCD band assignments for $[CrOCl_4]^-$ and $[MoOCl_4]^-$ and compares them to the values predicted from DVXα[51,52] and MSXα[54] calculations. The MCD assignments agree well with the DVXα transition energies including the assignment of CT bands at energies lower than the final ligand field transition. In fact, the largest discrepancies occur between the calculated and MCD transition energies for band 6 ($d_{xy} \rightarrow d_{z^2}$) where the DVX$\alpha$ values are approximately 3000 cm^{-1} lower than the MCD assignments. By way of contrast, the MSXα calculation predicts this transition to occur at higher energies.

While the spectra of the three complexes studied here display clear similarities in number of bands and in their relative positions, there are differences in the energies of these transitions which provide insight into the bonding at the metal center.

1.1. d_{xy} to d_{xz},d_{yz} Transitions. Band 1 is the d_{xy} to d_{xz},d_{yz} transition or a nonbonding to antibonding ($n \rightarrow \pi^*$) excitation. The energy at which band 1 is observed varies little in these complexes, changing only 1500 cm^{-1}, with the transition for $[WOCl_4(H_2O)]^-$ lying 700 cm^{-1} lower in energy than that for $[MoOCl_4]^-$. This insensitivity to the metal center has been commented on previously.[37] The short metal–oxygen distances in these complexes indicate a strong axial bond, which is supported by the decrease in d_{xy} to d_{xz},d_{yz} transition energy when a ligand trans to the oxygen is present in the compound (15 400 cm^{-1} for $[MoOCl_4]^-$, 14 400 cm^{-1} for $[MoOCl_5]^{2-}$, and 13 400 cm^{-1} for $[MoOCl_4(H_2O)]^-$).[20,36,53,63] SCF–MS–Xα calculations indicate that the energy of this transition is dependent on the ligand–metal–oxygen bond angle and on the metal–oxygen bond length.[40] For the $[MOCl_4]^-$ compounds the M–O–Cl bond angle changes very little (104.5(1)° for Cr to 105.3(2)° for W) while the metal–oxygen bond lengthens from 1.519(12) Å for Cr to 1.676(7) Å for W.[23, 64] Addition of an axial ligand both lengthens the M–O bond length (1.610(10) Å for $[MoOCl_4]^-$ vs 1.672(15) Å for $[MoOCl_4(H_2O)]^-$) and decreases the O–M–Cl bond angle (105.2(1)° for $[MoOCl_4]^-$ vs 99.0(9)° for $[MoOCl_4(H_2O)]^-$) as expected.[20,24] From this information, it appears that the changes in energy are due to variations in the M–O bond strength.

The difference between the excited-state and ground-state M–O stretching frequencies reflects increased antibonding character in the excited state. For the complexes considered here, the energy of the M–O stretch in the ground state is 1019 cm^{-1} ($[CrOCl_4]^-$) > 1012 cm^{-1} ($[MoOCl_4]^-$) > 980 cm^{-1} ($[WOCl_4(H_2O)]^-$) while the excited-state vibrational energies are 930 cm^{-1} (Cr) > 900 cm^{-1} (Mo) > 890 cm^{-1} (W). Since the difference in these values reflect the antibonding character, (112 cm^{-1} (Mo) > 90 cm^{-1} (W) ~ 89 cm^{-1} (Cr)) the greater magnitude of change for Mo relative to Cr and W indicates that the d_{xz},d_{yz} excited state for $[MoOCl_4]^-$ is slightly more antibonding relative to the Cr and W complexes, mirroring the electronic transition sequence. The position of $[WOCl_4(H_2O)]^-$ in this sequence is not unusual since the presence of the second axial group weakens the metal–oxygen bond and the ground-state M–O(OH_2) bond for these compounds is considered to be antibonding in nature.[52]

The vibrational data show that the d_{xz},d_{yz} orbitals are slightly more antibonding for Mo than W and Cr and excitation of an electron into the ^2E (d_{xz},d_{yz}) state alters the Mo–O bond strength the most, causing the largest change in M–O distance. That the transition from d_{xy} to d_{xz},d_{yz} occurs at roughly the same energy in Mo as it does in Cr and W even though the ^2E state is more antibonding for Mo implies that there must be a compensating shift in energy of the ground-state d_{xy} orbital between the two complexes. This greater destabilization of the d_{xy} orbital may arise from enhanced interactions between this orbital and equatorial ligand p orbitals or may derive from greater overlap with the oxygen.

1.2. d_{xy} to $d_{x^2-y^2}$ Transitions. In contrast to the d_{xy} to d_{xz},d_{yz} excitations, transitions from d_{xy} to $d_{x^2-y^2}$ (band 2) vary significantly with the metal center from 17 550 cm^{-1} for Cr(V) to 26 700 cm^{-1} for W(V). This transition involves excitation from a nonbonding orbital to an equatorial antibonding orbital ($n \rightarrow \sigma^*$) and corresponds to $\Delta 10Dq$ for these compounds. The changes in energy of this transition are thus proportional to Z_{eff} and vary as expected from the spectrochemical series.

2. Charge Transfer Manifold. The charge transfer(CT) manifold in these compounds consists of bands 3–7. Unlike the

---

(61) Seddon, K. R.; Thomas, V. H. *J. Chem. Soc., Dalton Trans.* **1977**, 2195.

(62) Collin, R. J.; Griffith, W. P.; Pawson, D. *J. Mol. Struct.* **1973**, *19*, 531.

(63) Wentworth, R. A. D.; Piper, T. S. *J. Chem. Phys.* **1964**, *41*, 3884.

(64) Fenske, D.; Stahl, K.; Hey, E.; Dehnicke, K. *Z. Naturforsch.* **1984**, *39b*, 850.

ligand field transitions, many of these bands collectively change energy together with variation in the metal center. The CT bands for the complexes increase in energy from $[CrOCl_4]^-$ to $[WOCl_4(H_2O)]^-$. Thus, the CT manifold for W looks similar to that found for Cr except that the W bands lie an average of some 12 700 cm^{-1} above the corresponding bands in the Cr complex. This trend can be explained by the increase in the first ionization energy from W to Cr.

Within the CT manifold, the splitting between bands 4 and 5 remains relatively constant at 2250 ± 100 cm^{-1} for $[MoOCl_4]^-$ and $[CrOCl_4]^-$. The energy separation between bands 3 and 5 for the Mo and Cr compounds also remains relatively unchanged at 4600 ± 300 cm^{-1}. Because these transitions arise from nonbonding orbitals consisting of Cl p orbitals, the variation in energy splitting is not unexpected. By way of contrast, the energy separation between bands 4 and 5 is 4000 cm^{-1} and between bands 3 and 5 is 5800 cm^{-1} for $[WOCl_4(H_2O)]^-$. The greater separation in these transitions with respect to the Cr and Mo complexes is due to the presence of the axial aqua ligand. The additional ligand decreases the O–M–Cl bond angle and changes the M–Cl overlap, which in turn alters the transition energies.

3. Evaluation of Ground-State Parameters. Definitive assignments of the optical bands enables us to understand the electronic structural origin of the ground-state EPR parameters for the complexes. EPR spectra for the $[MOCl_4]^-$ complexes have been recorded previously.[21,40,65] These complexes display an inverted EPR spectrum with $g_\parallel$ values greater than $g_\perp$. In addition, $g_\parallel$ for $[CrOCl_4]^-$ exceeds the free electron g value of 2.0023 while the $[MoOCl_4]^-$ $g_\parallel$ value approaches it. If the d orbital manifold alone is considered in calculating the g values, then, to first order, $g_\parallel = 2 - 8\lambda_M\alpha^2/\Delta E(d_{xy} \rightarrow d_{x^2-y^2})$ and $g_\perp = 2 - 2\lambda_M\alpha^2/\Delta E(d_{xy} \rightarrow d_{xz},d_{yz})$ where λ_M is the spin–orbit coupling constant for the metal and α^2 is the amount of metal d character. The only way in this formalism that $g_\parallel$ can be greater than $g_\perp$ and approach 2.00 with these metal centers is with substantial covalent delocalization over ligand centers with negative coupling constants, i.e. the O and Cl ligands. We would require some 89% ligand character in the ground-state d_{xy} orbital for Mo and 75% for W. This is inconsistent with the 80% W character in the first ^2E excited state determined from the reduction in in-state spin–orbit coupling from the free atom described above.

More detailed expressions for the g values are given below[40,66] with $\Delta_\parallel = g_e - g_\parallel$ and $\Delta_\perp = g_e - g_\perp$

$$\Delta_\parallel(b_1) = \frac{2(2\beta_1\epsilon_1\lambda_M - 4\beta_2\epsilon_3\lambda_L)(2\beta_1\epsilon_1 - 4\beta_2\epsilon_3)}{\Delta E(b_2(d_{xy}) \rightarrow b_1(d_{x^2-y^2}))} \qquad (1)$$

$$\Delta_\parallel(b'_1) = \frac{-2(2\beta_1\epsilon'_1\lambda_M + 4\beta_2\epsilon'_3\lambda_L)(2\beta_1\epsilon'_1 - 4\beta_2\epsilon'_3)}{\Delta E(b_2(d_{xy}) \rightarrow b_1(CT))} \qquad (2)$$

$$\Delta_\perp(e) = \frac{2(\alpha_3\beta_1\lambda_M + 2\alpha_{10}\beta_2\lambda_L)(\alpha_3\beta_1 + 2\alpha_{10}\beta_2)}{\Delta E(b_2(d_{xy}) \rightarrow e(d_{xz},d_{yz}))} \qquad (3)$$

Here β_1 and β_2 are the coefficients of the metal d and the halogen $p_{x,y}$ orbitals in the $2b_2$ molecular orbital, respectively; ϵ_1 and ϵ_3 are the corresponding coefficients for the ligand field $4b_1$ orbital; α_3 and α_{10} are the metal d_{xz},d_{yz} and halogen p_z orbital coefficients of the ligand field 7e orbital, respectively; ϵ_1' and ϵ_3' are the coefficients of the metal d and halogen $p_{x,y}$ orbitals of the highest lying filled b_1 orbital, respectively. The one-electron spin–orbit coupling constants for the metal d and halogen p orbitals are given by λ_M and λ_L, respectively. Excitation energies are denoted by ΔE. The additional term for $\Delta_\parallel$ arises from the charge transfer excited state of b_1 symmetry and contributes oppositely to the g value from the ligand field component because this latter excited state represents a bonding rather than antibonding state.

Application of this formalism using only the ligand field contributions (eqs 1 and 3) to the $[VOCl_4]^{2-}$ system yields values in very good agreement with experimental values.[40] However, the EPR spectrum for $[VOCl_4]^{2-}$ is not inverted and the lowest energy b_1 charge transfer band is at significantly higher energies than observed for the compounds considered here.[40,67] Equation 2 includes the contributions from all occupied orbitals of b_1 symmetry. From these equations, the negative shift in $g_\parallel$ from the ligand ($\Delta_\parallel(b_1)$) is offset by the positive contribution from the charge transfer $^2B_1$ level ($\Delta_\parallel(b_1')$). Since experimentally the ligand field and CT levels are displaced almost equally in magnitude from the ground state d_{xy} orbital, they almost exactly cancel each other. Sunil, Harrison, and Rogers[40,66] have made a similar argument based on theoretical considerations alone; this work confirms their insight experimentally. The $g_\parallel$ values close to the free electron value are then seen as a consequence of this low-lying b_1 charge transfer level as well as covalent delocalization in the ground state.

In order to test this insight, EPR parameters were computed using the bonding coefficients determined by the SCF–MS–Xα calculations of Sunil, Harrison, and Rogers[66] for $[CrOCl_4]^-$, those from Weber and Garner[54] for $[MoOCl_4]^-$, and the experimentally determined transition energies. For both compounds, the values of $g_\parallel$ and $g_\perp$ calculated using our transition energies (Mo, $g_\parallel = 1.957$, $g_\perp = 1.952$; Cr, $g_\parallel = 2.004$, $g_\perp = 1.979$) agree very well with the experimental values (Mo, $g_\parallel = 1.967$, $g_\perp = 1.950$; Cr, $g_\parallel = 2.006$, $g_\perp = 1.979$). In the Xα calculations only 15% covalent delocalization onto the equatorial Cl ligands in the ground state was obtained for both Mo and Cr. That this small degree of covalency can reproduce the inverted EPR g values indicates that covalency considerations are not solely responsible for the anomalous ground-state parameters. The low-lying b_1 CT level is very significant in manifesting $g_\parallel$ values close to 2.0023.

4. Comparison with Proteins. Optical spectra of the Mo-containing hydroxylases are likely to contain significant charge transfer contributions from equatorial sulfur ligands thought to be present in these systems. These CT components may be at energies lower than those in the model systems discussed here, especially if sulfur is present in the first coordination sphere as is thought from EXAFS[8,14,68,69] measurements. Preliminary data from $[MoO(SR)_4]^-$ complexes reveals a complex band structure centered around 18 000 cm^{-1} consisting of both ligand field and CT transitions. Spectra from DMSO reductase, a Mo enzyme which contains no other metals, reveal a rich band structure throughout the visible and near-infrared region.[17–19,70–72] The presence of the low-lying CT transition complicates spectral analysis and implies that conclusions based on shifts in broad transition manifolds should be made with caution. More generally, our assignment of the visible region ligand field and CT bands provides a necessary foundation for analysis of the features in the Mo-containing hydroxylases.

Our insight into the electronic structural origin of the ground state parameters in the model systems also complicates parallel analysis in the proteins. Like the $[MOCl_4]^-$ compounds, many of the molybdoenzymes display an inverted EPR where $g_\parallel$ is larger than $g_\perp$. In sulfite oxidase, for example, $g_\parallel = 2.0037$ and $g_\perp =$

---

(65) Garner, C. D.; Hyde, M. R.; Mabbs, F. E. *Inorg. Chem.* **1976**, *15*, 2327.
(66) Sunil, K. K.; Harrison, J. F.; Rogers, M. T. *J. Chem. Phys.* **1982**, *76*, 3078.
(67) Ballhausen, C. J.; Gray, H. B. *Inorg. Chem.* **1962**, *1*, 111.
(68) George, G. N.; Cleland, W. E.; Enemark, J. H.; Smith, B. E.; Kipke, C. A.; Roberts, S. A.; Cramer, S. P. *J. Am. Chem. Soc.* **1990**, *112*, 2541.
(69) Bray, R. C.; George, G. N. *Biochem. Soc. Trans.* **1985**, *13*, 560.
(70) Sabel, D. M.; Gewirth, A. A. Presented at the 201st National Meeting of the American Chemical Society Atlanta, Georgia; April, 1991.
(71) Thomson, A. J. Presented at the Fifth International Conference on Bioinorginic Chemistry, Oxford, U.K.; August, 1991.
(72) Johnson, J. L.; Rajagopalan, K. V. Presented at the 204th National Meeting of the American Chemical Society Washington D.C.; August, 1992.

1.9689 at low pH.[73] This may signify that low-energy charge transfer transitions are present and must be taken into account when determining the origin of the EPR signal.

VI. Conclusion

We have utilized MCD spectroscopy to provide a consistent assignment of ligand field and charge transfer bands in $[MOCl_4]^-$ complexes. We found that the ligand field energy ordering is $d_{xy} < d_{xz},d_{yz} < d_{x^2-y^2} < d_{z^2}$ and have also assigned the low-energy CT region of the spectra. This assignment aids in the understanding of the unique ground state parameters in these complexes. The $g_\|$ values close to 2.00 derive only slightly from covalent delocalization over ligands and mainly from the effect of low-lying B_1-symmetry CT bands. While spectra from Mo-containing enzymes are now becoming available, insight into EPR and visible spectra from these will require detailed study of additional model systems.

Acknowledgment. We thank Prof. John Enemark for helpful discussions. D.M.S. acknowledges a University of Illinois/Department of Education fellowship in chemistry. A.A.G. acknowledges a Presidential Young Investigator Award with matching funds made available by Digital Instruments, Inc. and is an A. P. Sloan Foundation Fellow. The Cary 14 spectrometer was generously made available by Dr. Gregorio Weber. Acknowledgment is made to the donors of The Petroleum Research Fund, administered by the American Chemical Society, for support of this research.

---

(73) Lamy, M. T.; Gutteridge, S.; Bray, R. C. *Biochem. J.* **1980**, *185*, 397.